A0026/77

JUN,1977

ANALYSIS OF INTERMEDIATE-ENERGY (γ,n) REACTIONS IN COMPLEX NUCLEI(*)

H.G. de Carvalho, M. Foshina and J.D. Pinheiro Filho(**)
Centro Brasileiro de Pesquisas Físicas, Rio de Janeiro, Brasil

and

V. di Napoli, J.B. Martins(***), F. Salvetti, O.A.P. Tavares(***)
and M.L. Terranova
Istituto di Chimica Generale ed Inorganica dell'Università, Roma

ABSTRACT

An analysis of the available experimental data on (γ,n) reaction cross sections at intermediate energies was made in order to obtain their dependence on the mass number A_t. The results were compared with those obtained by means of a Monte Carlo calculation based on photon-initiated intranuclear cascades. A relation has been established between the cross sections of elementary processes (pion photoproduction on single nucleon and Levinger's quasi-deuteron photodisintegration) and the (γ,n) probability. Cross section formulas have been obtained which give an A_t-dependence of the type aA_t^b, with b = 0.86 and a approximately equal to the cross sections of the elementary processes $\gamma + n \rightarrow n + \pi^0$ and $\gamma + p \rightarrow n + \pi^+$. These formulas reproduce almost all known experimental cross sections within a factor of 2, which seems to be rather good accuracy in view of the large range covered by both cross sections values and target mass numbers.

(*) Based on part of the Doctoral Thesis presented by J.B. Martins at the Centro Brasileiro de Pesquisas Físicas, Rio de Janeiro, November 1974. This work has been supported in part by the Brazilian Comissão Nacional de Energia Nuclear and by the Italian Consiglio Nazionale delle Ricerche.

(**) Permanent Address: Instituto de Física, Universidade Federal Fluminense, Niterói - RJ, Brasil.

(***) Permanent Address: Centro Brasileiro de Pesquisas Físicas, Rio de Janeiro, Brasil.

1. Introduction

Above about 0.1 GeV photons interact with nuclei giving rise to different kinds of reactions such as direct reactions , fragmentation, spallation and fission.

Direct reactions originate from the ejection from the struck nucleus of a very small number of nucleons and/or pions leading to a residual nucleus with an excitation energy not sufficient to "evaporate" other particles. Such reactions may be ascribed to a fast process that does not affect the rest of the nucleus. The (γ,n) and (γ,p) reactions are among the most remarkable examples of these processes.

In the region of intermediate energies (0.1-1.0 GeV) two models have successfully been proposed in order to explain the photon-nucleus interaction pattern: the Levinger's quasideuteron [1] and the photomesonic [2] interaction mechanisms. Following the quasideuteron model, the photon is absorbed by a neutron-proton pair within the nucleus and the cross section of most processes is strictly related to that of the deuteron photodisintegration, σ_d , and to the number of "quasideuterons" in the target nucleus. The quasideuteron contribution is important at energies up to 0.5 GeV, and becomes negligible above this energy value, due to the smallness of the cross section of the deuteron photodisintegration.

At incident energies higher than or equal to the threshold of π-meson photoproduction on single nucleons (about 0.15 GeV) , the experiment shows that the slopes of the yield curves become steeper the higher is the energy of the incoming photon, and broad resonances have been observed corresponding to the resonances found for single and double pion photoproduction. Another mechanism

of absorption has to be invoked, therefore, which is related to the pion photoproduction. Photonuclear cross sections must hence be connected with the total inelastic cross section, σ_{π} , of the γ-nucleon interaction.

The photomesonic model suggests, as the primary interaction, the photoproduction of a real or virtual π-meson from a single nucleon, followed by the two-step cascade-evaporation processes [2-5] . This mechanism becomes dominant as the energy increases.

Direct reactions, such as (γ,n), represent a rather conspicuous contribution to the total γ-nucleus inelastic cross section. As a consequence, knowledge of the dependence of the (γ,n) cross section on such parameters as photon energy and target mass number can give valuable information about some scarcely known aspects of photon absorption and clarify, to some extent, the mechanism of the interaction of photons with complex nuclei.

Since the experiment made by Baldwin and Klaiber [6] in 1948 using bremsstrahlung from the General Electric 100-MeV Betatron to measure the yields of $^{12}C(\gamma,n)^{11}C$ and $^{63}Cu(\gamma,n)^{62}Cu$ reactions, many attempts have been made to measure photoneutron cross sections covering very wide ranges of either energies and mass number of target nuclei.

The present status of measurements of single-neutron photoproduction cross section is characterized by a striking difference in the number of experiments, those made at the lower energies being considerably more numerous than at the intermediate and higher energies. Moreover, the use of almost monochromatic radiation produced by annihilation in flight of positrons, and of monochromatic gamma-rays from particle-induced reactions, has

provided a very large contribution to the comprehension of the low-energy processes, since it allows cleaner experiments than does the use of bremsstrahlung. Excellent review articles collect all known data on photoneutron cross section in the giant resonance region [7-9].

Unfortunately, the same is not true of the high-energy reactions, for which almost monochromatic beams have not yet extensively used for a number of reasons.

From all these facts it is readly understood how relatively poor information is presently available on (γ,n) reactions at energies above 0.1 GeV for both the scarcity of experimental data and the considerable conflict that there exists among the results from different laboratories. As far as this conflict is concerned, one should keep in mind that the cross sections given by the different authors are in general mean cross sections calculated from bremsstrahlung yield curves over wide energy ranges, and the difficulties inherent in using a bremsstrahlung spectrum to excite a nuclear reaction very often prevent one from observing a finer structure of these curves. On the other hand, whatever the method of computation, small changes in the yield curve can introduce large fluctuations in the calculated cross sections [10].

A number of papers have been published [11-33] on (γ,n) reactions in light and more complex nuclei in the energy range 0.1-1.0 GeV. In spite of the above-mentioned discrepancies, a general trend of increasing cross section with increasing mass number of the target nucleus can be deduced from the analysis of the data published in the literature from 1964 onward.

Some effort has been made to relate the (γ,n) cross sections to that of pion photoproduction. de Carvalho and cowor

kers [16] attempted to find a connection between the number of neutrons of the target nucleus, the cross section of pion photoproduction, and the transparencies of the nucleus to pions and recoil nucleons. Calculated values of nuclear transparencies [34,35], however, did not entirely corroborate this point of view,especially in the case of medium-weight and heavy nuclei, and the conclusion was drawn that the cross sections calculated in this way represent only lower limits for the (γ,n) reactions.

Researchers at Lund [36,37] were able to relate the (γ,n) cross section to the number of loosely bound neutrons in a few upper shell ("valence neutrons") in the nucleus. However, their calculations were restricted to a small number of light nuclei only.

In recent years Monte Carlo calculations have been developed which also considered the (γ,n) reaction. One of these calculations covers the bremsstrahlung energy range 40-350 MeV [38], making thus impossible a comparison with the data from experiments at higher energies; the other [39] is restricted to one target nucleus only (^{197}Au) as far as the (γ,n) reaction is concerned, and the calculated yield does not seem to reproduce satisfactorily enough the experimental results.

The decision as to which method of adjustment and/or comparison of the experimental data is preferable depends on whether the method chosen is suitable in providing the most general understanding of the phenomenon under investigation or not. Also, it should be able to give rather detailed information about the mechanism effective in producing the reactions considered. Furthermore, a test of its suitability might be the accuracy with which a cross section of a (γ,n) reaction for any element can be calculated.

We believed that a very useful method would consist in handling the available data on (γ,n) reaction in a statistical way and then, from the gross trend thus deduced, inferring some relationships between nuclear parameters and γ-nucleus interaction cross sections on the basis of theoretical models.

Also, the aim of this work was to carry out a Monte Carlo calculation on the cross sections of (γ,n) processes for target mass numbers between 12 and 238, at photon energies from 0.2 GeV up to 1 GeV and to compare the experimental cross sections with the calculated ones.

It is to be hoped that a study along these lines will contribute to our understanding of direct reactions.

2. Statistical Treatment of the Available Data

A total of 29 noteworthy cross section measurements are available to date for the (γ,n) reaction at energies between 0.1 GeV and 1.0 GeV. They regard 14 different target nuclei, rather well distributed throughout the periodic table.

In some cases only bremsstrahlung activation yield curves have been published, therefore the absolute cross sections (per photon) have been calculated by drawing least squares fits through the experimental yield values and by assuming a pure $1/k$ dependence of the bremsstrahlung spectra upon the photon energy k.

Before entering into a more detailed discussion on the experimental data and their arrangement, we believe it worthwhile to make some specifications about the symbolism used. Yields are expressed as cross sections per equivalent quantum and denoted

by the symbol σ_Q. The σ_Q values are functions of the bremsstrahlung end-point energy E_o. The cross section per photon, σ_k, also denoted as "absolute cross section", depends on the photon energy k.

The relation between $\sigma_Q(E_o)$ and $\sigma_k(k)$ is given by the integral equation of the type

$$\sigma_Q(E_o) = \frac{1}{Q} \int_o^{E_o} \sigma_k(k) n(k,E_o) dk \quad , \qquad (1)$$

where Q is the number of "equivalent quanta" (which represents the number of fictitious photons we should have if all the incident energy were equally distributed between photons of the maximum energy E_o) and $n(k,E_o)$ is the spectral density distribution of the bremsstrahlun used. Since we are interested in the measurement of the mean values of σ_k in the energy range from about 0.1 GeV up to about 1.0 GeV (in most cases 0.3-1.0 GeV), $n(k,E_o)$ can be approximated as Q/k and, consequently, the mean cross section $\bar{\sigma}_k$ in the energy range E_o'-E_o'' can be expressed by

$$\bar{\sigma}_k = \frac{\sigma_Q(E_o'') - \sigma_Q(E_o')}{\ln(E_o''/E_o')} \quad , \qquad (2)$$

E_o'-E_o'' being an energy interval within which the trend of σ_Q versus $\ln E_o$ may be approximated by a straight line.

In evaluating the mean cross sections per photon, $\bar{\sigma}_k$, in such a way, one disregards, in some way, the background contribution to the measured yields due to the giant resonance region, which in the case of (γ,n) reactions is relevant. This contribution strongly depends on the actual shape of the bremsstrahlung used,

thus different experimental arrangements may lead to remarkable different values of the measured σ_Q cross sections. Besides, the exact knowledge of the shape of the (γ,n) cross section resonance curves in the low energy region is not so straightforward, since in most cases the reported curves (see, for instance, Ref. [9]) are the sum of (γ,n) and (γ,pn) processes. Also, the quasideuteron contribution from the end of the giant resonance up to about 70 MeV, is hardly evaluable. As a consequence, the low-energy tail contributes to an extent which is very difficult to be evaluate. We decided, therefore, to disregard such corrections and use Eq. 2 in calculating the mean cross sections in the energy range 0.3-1.0 GeV. Of course, the cross sections thus obtained are slightly overestimated, as will be proved by the results of the Monte Carlo calculation.

Table 1 reports the experimentally determined mean cross sections for each target nucleus, with the energy range covered by the measurements.

As a first approach, all these data were plotted against the target mass number, A_t, on a log-log graph and a straight line fitted to them by means of the least squares method [40]. Only two points were disregarded in this fit, in view of their very large deviation from the mean, namely, the cross sections relative to ^{14}N and ^{103}Rh. The extremely small value of the cross section of the $^{14}N(\gamma,n)^{13}N$ reaction finds an explanation in the low proton separation energy of ^{13}N (about 1.9 MeV) which makes ^{13}N very unstable to proton emission. A small energy transfer to the rest nucleus during the photon interaction may easily excite ^{13}N which will then decay to the stable ^{12}C nucleus. No explanations have been found for the very high value of the cross section of the

$^{103}Rh(\gamma,n)^{102}Rh$ reaction.

From the straight line, the following mass number dependence of the mean cross section $\bar{\sigma}_k$ was found

$$\bar{\sigma}_k = 0.104\ A_t^{0.81}\ \text{mb} \quad , \tag{3}$$

with a correlation coefficient $r = 0.80$.

The good correlation we obtained in Ref. [40] between the logarithm of $\bar{\sigma}_k$ and the logarithm of A_t, strongly suggested that a linear dependence between these two variables should have been valid. As a consequence, a more refined least squares analysis was carried out by using the method of successive iterations with data rejection, i.e., after each iteration, all those experimental points whose deviations from the calculated values were larger than two times the standard deviation were rejected. A total of four iterations was needed (for the 5th iteration, all the remainder points fell within two times the standard deviation), with only 20% of the experimental points having been rejected. A correlation coefficient $r = 0.94$ has been obtained in such a way. The deduced A_t-dependence of the calculated mean cross section <u>per</u> photon was found to be

$$\bar{\sigma}_F = (0.083 \pm 0.008)A_t^{(0.880\ \pm\ 0.012)}\ \text{mb} \quad , \tag{4}$$

where $\bar{\sigma}_F$ denotes, henceforth, the value calculated from this fit.

Both Equations 3 and 4 give an A_t-dependence of $\bar{\sigma}(\gamma,n)$ of type

$$\bar{\sigma} = aA_t^{\,b} \quad , \tag{5}$$

with the exponent b higher than 2/3 (which would arise from a

surface pion production model [41,42]). A recent paper [43] correlates the trend of direct reactions with a volume production model [44,45] and with more recent experimental data on pion photoproduction [46,47]. The same conclusions have been reached by Heimlich et al. [48] for the electroproduction of negative pions.

Figure 1 shows the trend of $\bar{\sigma}_F(\gamma,n)$ versus the target mass number, A_t, as calculated from Eq. 4. The straight line has been back-extrapolated up to $A_t = 1$ for reasons which will be clear in a next section of this paper. The shaded area represents two times the error in the calculated $\bar{\sigma}_F$ values, as deduced from the fit errors in the coefficients a and b. The figure also reports the experimentally determined cross sections for the sake of comparison.

The relationship between $\bar{\sigma}_F$ and A_t, found by a simple statistical treatment of the available experimental data, will be soon compared with trat obtained by a stochastic treatment of the interactions that lead to a (γ,n) reaction.

The next section will describe the essentials of the Monte Carlo calculation which has been performed in order to obtain the cross section of the (γ,n) reactions.

3. Use of the Monte Carlo Method in the Study of the (γ,n) Reaction

There are in the literature several papers concerning the use of the Monte Carlo method for intranuclear cascades initiated by high-energy incident protons on complex nuclei [49-52]. In the absence of self-consistent theories covering the field of high-energy nuclear reactions, the Monte Carlo method turned out to be

a powerful tool in obtaining a number of important nuclear parameters which characterize the post-cascade nucleus. However, in the case of photons as incident particles, only a few applications of this method have been developed [38,39,53,54]. As the elementary γ-nucleon (γ-quasideuteron) and the subsequent particle-nucleon collisions are at present well known, the Monte Carlo method is entirely adequate in estimating the yields of specific photoreactions. In fact, Barashenkov et al. [39] were successful in carrying out a Monte Carlo calculation of photon-induced intranuclear cascades. A satisfactory agreement was observed between calculated and experimental data.

In this section we describe briefly the successive steps of the Monte Carlo calculation used in order to obtain the probabilities of (γ,n) reactions for complex nuclei ranging between ^{12}C and ^{238}U, and for incident photons of intermediate energies (0.2-1.0 GeV).

3.1. The Nuclear Model

We assumed the target nucleus as described by a degenerate Fermi gas of nucleons confined within a nuclear potential spherically symmetric of radius given by $r_o A_t^{1/3}$. Different values of r_o were assumed according to the mass range of the target nucleus [55]: $r_o = 1.4$ fm for $A_t < 30$; $r_o = 1.3$ fm for $30 < A_t < 100$; and $r_o = 1.2$ fm for $A_t > 100$.

According to the Serber's model [3], the high-energy particle reaction can be described by two independent step mechanism. In the first one, a rapid intranuclear cascade is initiated by the incoming particle, and successive interactions take place

between individualized nucleons. In the course of the calculation, we assumed classical trajectories in describing the scattering between particles [56]. During the fast cascade stage, there is a possibility for some particles (nucleons and/or mesons), as well as some nucleon aggregates (nuclear clusters) [57], to escape the nucleus. Absorption of nucleons and reabsorption of mesons can also occur, thus resulting in a transfer of a fraction of the incident energy to the target nucleus. In the second step, the excited residual nucleus loses its energy by the evaporation of a number of particles until a cold spallation residual is reached [58]. For heavy nuclei, fission can also take place as a mechanism of de-excitation competitive with particle evaporation.

In the present calculation we have taken into consideration only the development of the fast cascade step, since it is expected that a (γ,n) reaction will take place during those intranuclear cascades which lead to residual nuclei with an excitation energy not so high as to permit the evaporation of other particles.

We considered the following primary interactions:

quasideuteron interaction

$$\gamma + (np) \rightarrow n + p \qquad (6)$$

photomesonic interactions

$$\gamma + n \rightarrow n + \pi^0 \qquad (7)$$
$$\gamma + n \rightarrow p + \pi^- \qquad (8)$$
$$\gamma + p \rightarrow p + \pi^0 \qquad (9)$$
$$\gamma + p \rightarrow n + \pi^+ \qquad (10)$$
$$\gamma + n \rightarrow n + \pi^+ + \pi^- \qquad (11)$$
$$\gamma + n \rightarrow n + \pi^0 + \pi^0 \qquad (12)$$
$$\gamma + n \rightarrow p + \pi^- + \pi^0 \qquad (13)$$
$$\gamma + p \rightarrow p + \pi^+ + \pi^- \qquad (14)$$
$$\gamma + p \rightarrow p + \pi^0 + \pi^0 \qquad (15)$$
$$\gamma + p \rightarrow n + \pi^+ + \pi^0 \qquad (16)$$

In writing Eq. 7-16 we disregarded the intermediate steps via the

formation of nucleon isobars, only taking into consideration the products of the decay of these isobars.

Being the mean-free-path of intermediate-energy photons in nuclear matter ($\sim$ 140 fm) large with respect to the nuclear sizes, we were led to consider the nucleus as transparent to photons and, therefore, look at each point of the whole nucleus as an equally probable primary interaction point source. For the sake of simplicity, a reduction of the spherical nucleus to a bidimensional geometry was made [49].

As has been pointed out by Gabriel and Alsmiller [38] it is very difficult to evaluate the number of quasideuterons within the nucleus when this latter is subdivided in three distinct regions having different nucleon densities. On the other hand, such a subdivision would lengthen to a very great extent the computing time for the calculation of the paths travelled by the meson and recoil nucleon or by the photodisintegrated nucleon pair within the nucleus in their escaping.

From the above considerations, we decided to treat the nucleus within the framework of a constant nucleon density.

The photoproduced particles which result from the primary interaction can yield different kinds of secondary reactions. We have taken into account the following ones

$$\mathcal{N} + \mathcal{N} \rightarrow \mathcal{N} + \mathcal{N} \tag{17}$$

$$\mathcal{N} + \mathcal{N} \rightarrow \mathcal{N} + \mathcal{N} + \pi \tag{18}$$

$$\pi + (\mathcal{N}\mathcal{N}) \rightarrow \mathcal{N} + \mathcal{N} \tag{19}$$

$$\pi + \mathcal{N} \rightarrow \pi + \mathcal{N} \tag{20}$$

as the more representative in describing the cascade step.

3.2. Input Information

The total cross sections for the primary interactions were taken from Refs. [1,59-62]. In contrast with the assumption of Gabriel and Alsmiller [38] who considered the Levinger's factor L as being a constant for all the nuclei under investigation, we assumed an A_t-dependence of L as indicated in Table 2. The angular distribution for the reactions (6) and (19) was considered isotropic in the center of mass (CM) system. The differential cross sections for reactions (7-10) are those reported in Refs. [59,63], while for reactions (17-20) are those of the paper of Metropolis et al. [50]. For interactions of type (18) we have made the assumption that the total momentum was equally distributed between the produced particles in the CM system. The mean-free-path of the various particles in the course of a cascade was calculated following Refs. [34,35]. The total cross sections used in calculating the various nucleon-nucleon collision probabilities were those of the paper of Bertini [51].

3.3. The Course of the Calculation

The calculation itself was performed following the general way described by Metropolis et al. [50]. Only events of the type

$$\gamma + {}^{A}_{Z}X \rightarrow {}^{A-1}_{Z}X + n \qquad (21)$$

leading to residual nuclei with an excitation energy below the appropriate cutoff energy (see Table 3) were recorded. As result, we obtained the different probabilities for the above reactions as

defined by the ratio between the number of interactions yielding one-neutron deficient residual nuclei and the total number of iterations. The standard treatment of each case, viz., a fixed incident photon energy on a fixed target nucleus, involved about ten thousand incident photons. About hundred cases were analysed in the present calculation. The following target nuclei were selected: ^{12}C, ^{19}F, ^{23}Na, ^{55}Mn, ^{103}Rh, ^{197}Au and ^{238}U. They were chosen in order to give a moderately good coverage over complex nuclei of the periodic table.

The choosing of the first interaction point, the type of interaction and, in the case of photomesonic interaction, the target nucleon, was performed following the general procedure described by Rudstam [49]. The dynamics of successive collisions was treated relativistically in the usual manner [64,65]. The distance of travel, d, of the various particles was determined according to

$$d = - \lambda(E_i) \ln \xi \quad , \qquad (22)$$

where ξ is a random number in the interval 0-1 and $\lambda(E_i)$ is the mean-free-path of the particle i with kinetic energy E_i in nuclear matter.

The calculation was carried out by using the IBM/370 computer of the CBPF. The general course of the calculation, described in detail in the fluxogram of Fig. 2, has been programmed for the cascade step of any type of photonuclear reactions. For simple (γ,n) reactions, two remarkable simplifications have been made. At incident energies higher than or equal to 0.2 GeV, the kinematics of the quasideuteron photodisintegration leads to a

neutron and a proton both with kinetic energies larger than the cutoff energy of the struck nucleus. In view of this, they either escape the nucleus simultaneously or, if one or both are absorbed, give to the nucleus an energy sufficient to permit the evaporation of other particles. In any case, an event different from (21) would be registered.

In the case of double-pion photoproduction a large amount of energy is generally transferred to the nucleus and this will result in the emission of a number of particles during the evaporation stage. As a consequence, the contribution of this process to the (γ,n) probability can be assumed as almost negligible.

4. Results of the Monte Carlo Calculation

4.1. (γ,n) Reaction Probability

We define the (γ,n) reaction probability, $\Phi_n(k,A_t)$, as the ratio of the (γ,n) reaction cross section to the total inelastic cross section. Of course, this probability is a function of the photon energy k and the target mass number A_t.

The values of Φ_n have been obtained by means of the procedure already discussed in the preceding section (3.3) and are listed in Table 4, which also reports the mean values $\overline{\Phi}_n$, averaged over the energy range 0.3-1.0 GeV.

In Fig. 3 the trends of Φ_n *versus* the photon energy for the nuclei ^{12}C and ^{238}U are shown. The curves exhibit very broad bumps centered around 0.5 GeV. The same behaviour is also observed for the remainder nuclei we considered.

Plotted in Fig. 4 are the mean values $\overline{\Phi}_n$, in the energy

range 0.3-1.0 GeV, as a function of the target mass number A_t. The straight line through the calculated points is a least squares fit which gives an A_t-dependence of the form

$$\bar{\Phi}_n\ (k,A_t) = 0.234\ A_t^{-0.14} \qquad (23)$$

with an estimated error in $\bar{\Phi}_n$ ranging between 3% (^{12}C) and 6% (^{238}U). By back-extrapolating the straight line one obtains the value for $A_t = 1$.

4.2. The (γ,n) Cross Section

Above the threshold of pion photoproduction, the (γ,n) cross section is related to the total inelastic cross section in the following way

$$\sigma(k,A_t) = \left[A_t\ \sigma_{\mathcal{N}\rho}\delta + L(N_tZ_t/A_t)\sigma_d\ \delta'\right]\Phi_n(k,A_t) \quad , \qquad (24)$$

where the expression in brackets represents the total inelastic cross section, which accounts for the photomeson (the first term in the sum) and the quasideuteron interaction mechanisms. The quantities δ and δ', which also depend on A_t and k, are factors related to the nuclear excitation, according to the type of interaction, and are very close to unity at energies below 1 GeV. The values of $\sigma_{\mathcal{N}\rho}(k)$ have been taken from Ref. [66] and those of $\sigma_d(k)$ from Ref. [1].

By using the ϕ_n probabilities of Table 4 we got the values of $\sigma(k,A_t)$ for (γ,n) reactions, which we shall denote by the symbol σ_{MC}, and are listed in Table 5.

In Fig. 5 the trends are reported of σ_{MC} for the two nuclei ^{12}C and ^{238}U.

By least squares fitting the mean values $\overline{\sigma}_{MC}$(0.3-1.0GeV) taken from Table 5, the straight line has been obtained which is shown in Fig. 6. The A_t-dependence of $\overline{\sigma}_{MC}$ has the following expression

$$\overline{\sigma}_{MC} = (0.063 \pm 0.006)\ A_t^{0.860 \pm 0.012}\ \text{mb} \ . \qquad (25)$$

Also in this case an exponent higher than 2/3 and very close to the exponent of Eq. 4 has been found.

5. Discussion

5.1. Comments on the Treatment of Experimental Data

The relatively large number of experimental data on the (γ,n) reaction, covering the regions of light ($12 \leq A_t \leq 31$), medium-weight ($31 < A_t \leq 103$) and heavy ($103 < A_t \leq 238$) nuclei, allowed a good statistical treatment to be made, which led to Eq. 4.

Only mean cross sections per photon were used, due to the lack of a large number of experimental values of cross sections per equivalent quantum at the different bremsstrahlung energies for each target nucleus. Owing to this fact, a square shape of the bremsstrahlung spectra has been assumed in calculating the mean cross sections per photons (see Eq. 2) and consequently these cross sections are slightly overestimated (see also section 2).

In the case of the $^{12}C(\gamma,n)^{11}C$ reaction, for which a larger number of experimental data were available, it was possible to determine the trend of σ_k as a function of the photon energy ,

by resolving Eq. 1 (see Ref. [27]). However, the resolution of this integral equation gives strongly oscillating solutions due to its mathematical structure [67].

We wish also to point out that, by extrapolating Eq. 4 to $A_t = 1$ a cross section value of 0.083 mb is obtained, which is very close to the mean cross section values of the elementary processes $\gamma + p \rightarrow n + \pi^+$ ($\bar{\sigma} = 0.070$ mb) and $\gamma + n \rightarrow n + \pi^0$ ($\bar{\sigma} = 0.096$ mb). Such an agreement can be considered reasonable if we recall the large errors involved in the primary cross section measurements and in the coefficient of Eq. 4.

5.2. A Deeper Insight into the (γ,n) Reaction Probability

Equation 23 of section 4.1 gives the A_t-dependence of the mean value of the (γ,n) reaction probability $\bar{\Phi}_n$. The coefficient 0.234 of Eq. 23 must represent the mean (γ,n) probability for a target having $A_t = 1$. For $A_t = 1$, two types of target have to be taken into consideration, i.e., either a proton target or an (idealized) neutron target and therefore the interactions we must consider are the following

$$\gamma + p \rightarrow n + \pi^+ \qquad \text{(proton target)} \qquad (26)$$

and

$$\gamma + n \rightarrow n + \pi^0 \qquad \text{(neutron target)} \qquad (27)$$

In both cases, in fact, the photoproduction of a single neutron is obtained.

The mean probabilities of these processes are obtained from the mean ratios between the cross sections of each process and the total inelastic cross section per nucleon, via the photo

mesonic mechanism of interaction. These ratios are found to be 0.36 and 0.24, respectively, and are in good agreement within the limits of errors, which are quite large, with the value 0.234 arising from Eq. 23 (see Fig. 4). One should consider, though, that the first elementary process showed above (Eq. 26) is effective in giving a direct (γ,n) reaction for $A_t = 1$ solely, since for $A_t > 1$ it may contribute to the (γ,n) reaction only through an indirect way. On the contrary, the other process (Eq. 27) will contribute in any case to the (γ,n) reaction. As a matter of fact, we found an extrapolated value which is very close to the mean calculated probability for the second process. This result is easily explained if one keeps into consideration the higher escaping probabilities of uncharged particles.

As has already been said, the (γ,n) probability Φ_n is a function of the target mass number and photon energy. Let us write this function as

$$\Phi_n(k,A_t) = \phi(A_t)\eta(k) \quad , \tag{28}$$

i.e., as the product of two functions, each depending on one variable only. Further, let us assume $\phi(A_t)$ be of the form

$$\phi(A_t) = A_t^{\alpha} \quad .$$

In this way, Eq. 28 becomes

$$\Phi_n(k,A_t) = A_t^{\alpha}\,\eta(k) \quad . \tag{29}$$

By using for $\bar{\sigma}(\gamma,n)$ the expression of Eq. 24, we obtain

$$\bar{\sigma}(\gamma,n) = \left\langle \left[A_t\,\sigma_{\mathcal{N}} + L\,\frac{N_t Z_t}{A_t}\,\sigma_d \right] \Phi_n(k,A_t) \right\rangle \quad . \tag{30}$$

Being $N_t Z_t / A_t$ roughly approximated by $0.25\ A_t$, and the Levinger's factor by $L = 2.68\ A_t^{0.28}$ (see Ref. [40]), Eq. 30 becomes

$$\bar{\sigma}(\gamma,n) = A_t \left\langle \left[\sigma_{\mathcal{N}} + 0.67\ A_t^{0.28}\ \sigma_d \right] \Phi_n(k,A_t) \right\rangle \qquad (31)$$

and substituting $\Phi_n(k,A_t)$ from Eq. 29 gives

$$\bar{\sigma}(\gamma,n) = A_t^{\alpha+1} \left\langle \left[\sigma_{\mathcal{N}} + 0.67\ A_t^{0.28}\ \sigma_d \right] \eta(k) \right\rangle \quad . \qquad (32)$$

At this point, we can disregard the second term in the expression within brackets, since it represents only 5% of $\sigma_{\mathcal{N}}$ for ^{12}C and 12% for ^{238}U, thus obtaining

$$\bar{\sigma}(\gamma,n) \simeq A_t^{\alpha+1} \left\langle \sigma_{\mathcal{N}}(k)\eta(k) \right\rangle \quad , \qquad (33)$$

$\langle \sigma_{\mathcal{N}}(k)\eta(k) \rangle$ being now a function of the photon energy only. By comparing Eq. 33 with Eq. 25, it can be written with a satisfactory degree of approximation

$$\begin{cases} \langle \sigma_{\mathcal{N}}(k)\eta(k) \rangle = 0.063 \text{ mb} \\ \alpha + 1 = 0.86 \end{cases} \qquad (34)$$

whence, $\alpha = -0.14$.

Finally, Eq. 29 may be rewritten as

$$\Phi_n(k,A_t) = A_t^{-0.14}\ \eta(k) \qquad (35)$$

from which

$$\eta(k) = \Phi_n\ A_t^{0.14} \quad . \qquad (36)$$

Values of $\eta(k)$ have been calculated for different nuclei, as a

function of the photon energy, by means of Eq. 36 and by using for Φ_n the values listed in Table 4. At each energy $\eta(k)$ was in effect found approximately constant for all target nuclei under investigation, thus supporting the idea of considering η as a function of the photon energy only.

In Fig. 7 the trend of η/k is shown as a function of the photon energy. By least squares fitting the points in the figure a straight line has been drawn from which the following equation is obtained

$$\eta(k) = 1.25\ k \exp\left[-k/0.55\right] \quad , \qquad (37)$$

k being expressed in GeV. The function η reachs its maximum at 0.55 GeV. This means that the (γ,n) probability should also reach a maximum at the same energy. This behaviour has already been found for Φ_n , as shown in Fig. 3. An explanation of such a trend may lie in the fact that the mean-free-path of the photo-produced particles increases from 0.3 GeV up to about 0.5 GeV, and the increased mean-free-path enhances the probability of a (γ,n) reaction via a direct process. Above about 0.5 GeV the double-pion photoproduction, instead, lowers considerably this probability, since this process certainly contributes to the total inelastic cross section but it does not contribute markedly to the (γ,n) process in view of the high excitation energy given to the nucleus.

The mean value of η between 0.3 GeV and 1.0 GeV turns out to be 0.237 which agrees quite completely with 0.234 of Eq. 23 for $A_t = 1$ (see also Eq. 36).

5.3. Comparison Between Experimental and Calculated (γ,n) Cross Sections

The most general relationship between the (γ,n) reaction

cross section and the total inelastic cross section is given by Eq. 24, which is valid for any target nucleus and for energies above the giant resonance region.

By means of the Monte Carlo method we succeded in calculating the (γ,n) probability $\Phi_n(k,A_t)$ and thus in deducing the cross sections of (γ,n) reactions. These values, listed in Table 5, are shown in graphical form in Fig. 5, where the trends for ^{12}C and ^{238}U only are reported for the sake of clearness. Figure 5 also reports the trend of $\sigma(\gamma,n)$ for ^{12}C taken from Ref. [27]. A satisfactory agreement between the calculated and experimental curves has been found.

A more simplified expression of $\sigma(\gamma,n)$ can be established by disregarding the quasideuteron contribution to the total inelastic cross section and by using Eqs. 35 and 37, which give

$$\sigma_C(\gamma,n) = 1.25\ \sigma_{\mathcal{N}} \rho k \exp\left[-k/0.55\right] A_t^{0.86} \text{ mb} \quad (k \text{ in GeV}) , \quad (38)$$

where σ_C denotes the cross section calculated in this way.

Mean values of the cross sections <u>per</u> photon of the (γ,n) reaction have been calculated by means of Eq. 4 (least squares fit of the experimental data), Eq. 24 (Table 4), and Eq. 25 (least squares fit of the Monte Carlo calculated points). We also calculated the mean cross sections <u>per</u> photon by means of Eq. 38. The results are summarized in Table 6.

From the analysis of Table 6 it can be concluded that only a few experimental values are not well reproduced by the calculated cross sections, namely, ^{14}N [23], ^{55}Mn [17], ^{75}As [22], ^{103}Rh [19] and ^{127}I [14]. In the other cases, experimentally determined cross sections are reproduced within a

factor less than or equal to two.

The fact that the accuracy in predicting (γ,n) cross sections varies within a factor two might seem to be rather a bad agreement, but it should be remembered that the range of values covered is quite large (a factor of more than 25) and the same is true of the range of nuclear masses (10-240). Moreover, the experimentally determined cross sections are quite often very uncertain and the precision with which the four different equations (Eqs. 4, 24, 25 and 38) predict (γ,n) cross sections is probably better than the uncertainty factors would indicate.

5.4. Mass Number-Dependence of the Cross Sections

A number of papers attempted to correlate the yield of pion photoproduction with the mass number of the target nucleus. Early measurements of charged pion photoproduction from nuclei showed an $A_t^{2/3}$-dependence of the cross sections upon the target mass number A_t and this dependence was related [41,42] to a surface production mechanism (surface production model). Further experiments have shown, on the contrary, that the phenomenon actually exhibits an $A_t^{3/4}$-dependence and this has led to a volume production model [43-45] which also accounts for a more or less strong reabsorption of pions within the nucleus.

More recent experiments [46-48] seem to confirm the predictions of the volume production model. Shramenko et al. [47], by using known values of nuclear transparencies [34,35], found an 0.88-dependence for the photoproduction of π^+- and π^--mesons.

Above about 0.2 GeV, a (γ,n) reaction may originate via the photomesonic interaction mechanism only, the quasideuteron

mechanism being energetically ineffective in producing a (γ,n) reaction.

Taking into account the primary interactions (7-16) listed in section 3.1, it is clear that both neutrons and protons do contribute to a (γ,n) reaction and thus the cross section of this process must depend on the mass number A_t and not on the neutron number N_t only.

By means of quite different method we obtained the following mass number dependences of $\bar{\sigma}(\gamma,n)$: $A_t^{0.88}$ from the statistical treatment of the experimental data and $A_t^{0.86}$ from the Monte Carlo calculation. The conclusion can be therefore drawn that also in this case, the volume production model is adequate in describing the mechanism of interaction leading to a (γ,n) reaction. Such a conclusion is clearly shown by the trends plotted in Fig. 6.

6. Conclusions

We wish to summarize briefly the most interesting results that have been obtained in the course of this work.

i) In spite of the fact that the Monte Carlo calculation has been carried out by using monoenergetic photons as incident particles, a good agreement has been found with the experimental mean cross sections deduced from bremsstrahlung yields.

ii) The cross sections of (γ,n) reactions increase with increasing the target mass number A_t in the energy range 0.3-1.0GeV.

iii) The (γ,n) reaction probability decreases with increasing the target mass number A_t in the same energy range.

iv) The (γ,n) reaction probability reachs a maximum at about 0.55GeV.

v) The quasideuteron mechanism of interaction does not contribute to the (γ,n) reaction at energies above 0.2 GeV.

vi) Double- and multiple-pion photoproduction play an almost negligible role in producing a (γ,n) reaction.

vii) Both neutrons and protons are sources of primary interactions which may lead to a (γ,n) process.

The present paper is only a part of a systematic work aimed to study in detail the (γ,xn) $(x \geq 1)$ reactions, as well as the $(\gamma,yp\ xn)$ (spallation) reactions with the aid of the Monte Carlo calculation. Future work will be devoted to the study of the (γ,xn) $(x > 1)$ reactions and the results will be the argument of further communications.

ACKNOWLEDGEMENT

The authors wish to acknowledge the tireless collaboration of the computer staff of the Centro Brasileiro de Pesquisas Físicas. J.B. Martins and O.A.P. Tavares wish to express their appreciation of the very kind hospitality they received from the Istituto di Chimica Generale ed Inorganica dell'Università di Roma.

REFERENCES

1. J.S. Levinger, Phys. Rev. 84, 43 (1951); 97, 970 (1955).
2. I. Reff, Phys. Rev. 91, 150 (1953).
3. R. Serber, Phys. Rev. 72, 1114 (1947).
4. M.L. Goldberger, Phys. Rev. 74, 1269 (1948).
5. C.E. Roos and V.Z. Peterson, Phys. Rev. 124, 1610 (1961).
6. G.C. Baldwin and G.S. Klaiber, Phys. Rev. 73, 1156 (1948).
7. B.M. Spicer, Suppl. Nuovo Cimento 2, 243 (1964).
8. B. Bülow and B. Forkman, Lund Preprint, to be published by A.B. Atomenergi, Studsvik, Sweden (ed. D. Brune).
9. B.L. Berman and S.C. Fultz, Rev. Mod. Phys. 47 (1975).
10. K. Tesch, Nucl. Instr. Methods 95, 245 (1971).
11. W.C. Barber, W.D. George and D.D. Reagan, Phys.Rev.98,73(1955).
12. A. Masaike, J. Phys. Soc. Japan 19, 427 (1964).
13. Yu. P. Antuf'ev, I.I. Miroschnichenko, V.I. Noga, P.V.Sorokin, Sov. J. Nucl. Phys. 6, 312 (1968).
14. G.G. Jonsson, B. Forkman, K. Lindgren, Phys. Lett. 26B, 508 (1968).
15. V. di Napoli, F. Dobici, O. Forina, F. Salvetti and H.G. de Carvalho, Nuovo Cimento 55B, 95 (1968).
16. H.G. de Carvalho, V. di Napoli, D. Margadonna, F. Salvetti and K. Tesch, Nucl. Phys. A126, 505 (1969).
17. G. Andersson, B. Forkman and B. Friberg, University of Lund Report Nº LUNP 6901, January 1969, p. 11 (unpublished).
18. G. Andersson and B. Forkman, University of Lund Annual Report 1969, Sect. 5-A: 1d.
19. V. di Napoli, D. Margadonna, F. Salvetti, H.G. de Carvalho and J.B. Martins, Lett. Nuovo Cimento 1, 308 (1969).
20. G.G. Jonsson, K. Lindgren and B. Forkman, University of Lund Report Nº LUNP 6901, January 1969, p. 14 (unpublished).

21. G. Hyltén, Nucl. Phys. A158, 225 (1970).

22. G. Andersson and B. Forkman, University of Lund Annual Report 1970, p. 48.

23. B. Friberg, G. Andersson, and B. Forkman, Nucl. Phys. A171 , 551 (1971).

24. V. di Napoli, D. Margadonna, F. Salvetti, H.G. de Carvalho and J.B. Martins, Nucl. Instr. Methods 93, 77 (1971).

25. K. Lindgren and G.G. Jonsson, Nucl. Phys. A166, 643 (1971).

26. V. di Napoli, F. Salvetti, H.G. de Carvalho and J.B. Martins, Lett. Nuovo Cimento 1, 538 (1971).

27. G. Andersson, I. Blomqvist, B. Forkman, G.G. Jonsson, A.Järund, I. Kroon, K. Lindgren, B. Schrøder and K. Tesch, Nucl. Phys. A197, 44 (1972).

28. B. Schrøder, B. Nordgren and A. Alm, University of Lund Report Nº LUNP 7206, March 1972, p. 17.

29. V. di Napoli and M.L. Terranova, Gazz. Chim. Ital. 103, 551(1973).

30. F. Salvetti, C. Aurisicchio, V. di Napoli, M.L. Terranova, H. G. de Carvalho and J.B. Martins, Gazz. Chim. Ital. 103, 1003 (1973).

31. H.G. de Carvalho, J.B. Martins, O.A.P. Tavares, V. di Napoli and F. Salvetti, Proc. Int. Conference on Photonuclear Reactions and Applications, Pacific Grove (Cal.), March 26-30 , 1973, Section 8C5-1.

32. V. di Napoli, M.L. Terranova, H.G. de Carvalho and J.B.Martins, Gazz. Chim. Ital. 104, 463 (1974).

33. V. di Napoli, F. Salvetti, M.L. Terranova, H.G. de Carvalho, J.B. Martins, and O.A.P. Tavares, Gazz. Chim. Ital. 105,67(1975).

34. H.G. de Carvalho, J.B. Martins, O.A.P. Tavares, R.A.M.S. Nazareth and V. di Napoli, Lett. Nuovo Cimento 2, 1139 (1971).

35. H.G. de Carvalho, J.B. Martins, O.A.P. Tavares, R.A.M.S. Nazareth and V. di Napoli, Lett. Nuovo Cimento 4, 365 (1972).

36. G. Andersson, B. Forkman and B. Friberg, University of Lund Report Nº LUNP 7010, September 1970.

37. G. Andersson, B. Forkman and B. Friberg, Nucl. Phys. A171 , 529 (1971).

38. T.A. Gabriel and R.G. Alsmiller, Jr., Phys. Rev. 182, 1035(1969).

39. V.S. Barashenkov, F.G. Gereghi, A.S. Iljinov, G.G. Jonsson and V.D. Toneev, Nucl. Phys. A231, 462 (1974).

40. V. di Napoli, F. Salvetti, M.L. Terranova, H.G. de Carvalho , J.B. Martins and O.A.P. Tavares, Gazz. Chim.Ital. 105,317(1975).

41. R.R. Wilson, Phys. Rev. 86, 125 (1952).

42. S.T. Butler, Phys. Rev. 87, 1117 (1952).

43. V. di Napoli, Lett. Nuovo Cimento 12, 609 (1975).

44. J.R. Waters, Phys. Rev. 113, 1133 (1959).

45. W.M. McClelland, Phys. Rev. 123, 1423 (1961).

46. G.N. Dudkin, V.N. Eponeshnikov, Yu. F. Krechetov and V.A. Tryasuchev, Kharkov Physico-Technical Institute Report Nº KFTI 73-31, p. 66 (1973) (in Russian).

47. B.I. Shramenko, I.A. Grishaev, V.I. Nikiforov and G.D.Pugachev, Kharkov Physico-Technical Institute, Report Nº KFTI 73-31, p. 74, (1973) (in Russian).

48. F.H. Heimlich, G. Huber, E. Rössle, P. David, H. Mommsen and D. Wegener, Nucl. Phys. A267, 493 (1976).

49. G. Rudstam in "Spallation of Medium-Weight Elements", Doctoral Thesis, NP 6191, University of Uppsala, Uppsala (1956).

50. N. Metropolis, R. Bivins, M. Storm, A. Turkevich, J.M. Miller, and G. Friedlander, Phys.Rev. 110, 185 (1958); N. Metropolis, R. Bivins, M. Storm, G.M. Miller, and G. Friedlander, Phys. Rev. 110, 204 (1958).

51. H.W. Bertini, Phys. Rev. 188, 1711 (1969).

52. V.S. Barashenkov, H.W. Bertini, K. Chen, G. Friedlander, G. D. Harps, A.S. Iljinov, J.M. Miller and V.D. Toneev, Nucl. Phys. A187, 531 (1972).

53. K.K. Gudima, A.S. Iljinov, and V.D. Toneev, JINR communications P2-4661, P2-4808, Dubna (1969).

54. N.L. Emetz, G. Ya. Lubarsky, Yu. N. Ranyuk, and P.V. Sorokin, Kharkov Physico-Technical Institute Report Nº KFTI 72-37 (1972) (in Russian).

55. L.R.B. Elton, Introductory Nuclear Theory, Ptman, London(1965).

56. P.A. Benioff, Phys. Rev. 119, 324 (1960).

57. V. di Napoli, F. Salvetti, M.L. Terranova, H.G. de Carvalho, and J.B. Martins, Phys. Rev. C8, 206 (1973).

58. V. Weisskopf, Phys. Rev. 52, 295 (1937).

59. J.T. Beale, S.D. Ecklund and R.L. Walker, Report CTSL-42 , CALT 68-108 (1968).

60. H.G. Hilpert et al., ABBHHM Collaboration, Nucl. Phys. B8 , 535 (1968).

61. C. Betourne, J.C. Bizot, J. Perez y Jorba, D. Treille, Phys. Lett. 24B, 590 (1967). See also other references quoted therein.

62. ABBHHM Collaboration, Phys. Rev. 175, 1669 (1968).

63. P. Spillantini and V. Valente, Report CERN-HERA 70.1 (1970).

64. K.G. Dedrick, Rev. Mod. Phys. 34, 429 (1962).

65. J.D. Jackson in "Classical Electrodynamics", John Wiley & Sons, London (1962).

66. M. Damashek and F.J. Gilman, Phys. Rev. D1, 1319 (1970).

67. D.L. Phillips, Journal A.C.M. 9, 84 (1962).

Table 1 - Mean Experimental Cross Sections for (γ,n) Reactions at Intermediate Energies

Target Nucleus	Energy Range (GeV)	Laboratory	Cross Section (mb)	Ref.
^{12}C	0.2 - 0.72	INS, Tokyo	0.85 ± 0.10	12
	0.3 - 1.4	PTI, UAS	0.4 ± 0.1	13
	0.3 - 1.0	Frascati	1.18 ± 0.20	15
	0.2 - 1.0	Lund	0.6 ± 0.1	21,27
	0.3 - 1.0	Frascati	0.9 ± 0.1	32
^{14}N	0.32 - 0.62	Lund	0.11 ± 0.05	23
^{16}O	0.3 - 0.8	Lund	0.6 ± 0.1	23
	0.3 - 1.0	Frascati	1.27 ± 0.20	29
^{19}F	0.3 - 0.9	Lund	0.42 ± 0.10	23
	0.3 - 1.0	Frascati	1.33 ± 0.20	24
	0.3 - 1.0	Frascati	1.30 ± 0.10	30
^{23}Na	0.3 - 1.0	Frascati	1.60 ± 0.20	30
^{31}P	0.3 - 0.8	Lund	0.9 ± 0.1	23
	0.3 - 1.0	Frascati	1.6 ± 0.1	32
^{52}Cr	0.3 - 1.0	Frascati	2.5 ± 0.5	33
^{55}Mn	0.1 - 0.8	Lund	7.7 ± 0.5	17
	0.3 - 1.0	Frascati	4.2 ± 0.6	31
	0.3 - 1.0	Frascati	3.5 ± 0.5	33
^{59}Co	0.2 - 0.8	Lund	3.3 ± 0.5	18
	0.3 - 1.0	Frascati	3.0 ± 0.5	33
^{75}As	0.3 - 0.9	Lund	8.7 ± 1.0	22
	0.3 - 1.0	Frascati	4 ± 1	33
^{103}Rh	0.4 - 0.9	Orsay	13 ± 5	19
^{127}I	0.15 - 0.80	Lund	10 ± 6	14
	0.1 - 0.8	Lund	4 ± 2	20
	0.3 - 1.0	Frascati	5 ± 2	33
^{197}Au	0.3 - 0.9	Lund	4 ± 2	25
	0.3 - 1.0	Frascati	8 ± 3	33
^{238}U ([a])	0.3 - 1.0	Frascati	10 ± 5	26

([a]) There is in literature another measurement of the reaction $^{238}U(\gamma,n)^{237}U$ (Ref. [28]), but the reported values are 13 ± 5 mb in the energy range 0.2-0.5 GeV and -4 ± 15 mb in the energy range 0.5-0.7 GeV.

Table 2 - Dependence of the Levinger's Factor, L, on the Mass Number, as Used in the Present Monte Carlo Calculation.

Nucleus	^{12}C	^{19}F	^{23}Na	^{55}Mn	^{103}Rh	^{197}Au	^{238}U
L	5.5	7	7	9	11	12	12

Table 3 - Values of the Cutoff Energy and Related Nuclear Characteristics Used in the Present Monte Carlo Calculation.(All Energies in MeV).

Nucleus	Fermi Energy		Average Binding Energy of Loosest Nucleon	Coulomb Energy at Surface	Cutoff Energy (*)
	Protons	Neutrons			
^{12}C	24.6	24.6	7.7	2.3	34.5
^{19}F	23.7	25.4	7.9	3.1	35.6
^{23}Na	23.9	25.3	8.3	3.6	36.5
^{55}Mn	23.1	26.1	8.7	6.5	39.8
^{103}Rh	26.1	30.9	8.6	10.4	47.5
^{197}Au	28.9	37.7	7.9	16.1	57.3
^{238}U	28.2	38.4	7.5	17.6	58.4

(*) The cutoff energy was calculated as the average Fermi energy of neutrons and protons plus the average binding energy of the loosest nucleon plus the Coulomb energy at surface.

Table 4 - The (γ,n) Reaction Probabilities, $\Phi_n(k,A_t)$, as Obtained by the Present Monte Carlo Calculations (*).

k(GeV)	^{12}C	^{19}F	^{23}Na	^{55}Mn	^{103}Rh	^{197}Au	^{238}U
0.20	0.007 ± 0.002	0.012 ± 0.003	0.012 ± 0.003	0.019 ± 0.004	0.025 ± 0.005	0.034 ± 0.005	0.038 ± 0.006
0.25	0.092 ± 0.009	0.079 ± 0.008	0.077 ± 0.008	0.062 ± 0.007	0.027 ± 0.005	0.052 ± 0.007	0.053 ± 0.007
0.30	0.152 ± 0.011	0.134 ± 0.010	0.130 ± 0.010	0.110 ± 0.009	0.096 ± 0.009	0.085 ± 0.008	0.085 ± 0.008
0.32	0.169 ± 0.011	0.147 ± 0.010	0.147 ± 0.010	0.116 ± 0.010	0.108 ± 0.009	0.091 ± 0.009	0.087 ± 0.008
0.35	0.162 ± 0.011	0.147 ± 0.010	0.149 ± 0.011	0.133 ± 0.010	0.116 ± 0.010	0.104 ± 0.009	0.101 ± 0.009
0.40	0.161 ± 0.011	0.141 ± 0.010	0.143 ± 0.010	0.154 ± 0.010	0.119 ± 0.010	0.106 ± 0.009	0.108 ± 0.009
0.45	0.180 ± 0.012	0.170 ± 0.011	0.170 ± 0.011	0.153 ± 0.011	0.135 ± 0.010	0.137 ± 0.010	0.139 ± 0.011
0.50	0.163 ± 0.014	0.147 ± 0.011	0.129 ± 0.011	0.136 ± 0.011	0.123 ± 0.010	0.114 ± 0.010	0.113 ± 0.011
0.55	0.173 ± 0.014	0.165 ± 0.012	0.166 ± 0.013	0.152 ± 0.012	0.145 ± 0.012	0.133 ± 0.012	0.129 ± 0.011
0.60	0.167 ± 0.014	0.163 ± 0.012	0.158 ± 0.013	0.139 ± 0.012	0.134 ± 0.012	0.119 ± 0.011	0.116 ± 0.011
0.65	0.158 ± 0.014	0.153 ± 0.013	0.149 ± 0.013	0.128 ± 0.012	0.123 ± 0.012	0.107 ± 0.011	0.107 ± 0.011
0.70	0.171 ± 0.014	0.163 ± 0.013	0.159 ± 0.013	0.139 ± 0.012	0.133 ± 0.012	0.114 ± 0.011	0.110 ± 0.011
0.80	0.167 ± 0.014	0.166 ± 0.013	0.164 ± 0.013	0.140 ± 0.012	0.125 ± 0.012	0.111 ± 0.011	0.107 ± 0.011
0.90	0.144 ± 0.014	0.137 ± 0.013	0.131 ± 0.013	0.114 ± 0.012	0.104 ± 0.012	0.085 ± 0.011	0.084 ± 0.011
1.00	0.148 ± 0.014	0.135 ± 0.012	0.135 ± 0.013	0.114 ± 0.012	0.108 ± 0.010	0.085 ± 0.010	0.082 ± 0.010
$\overline{\Phi}_n$ (**)	0.161 ± 0.013	0.151 ± 0.012	0.148 ± 0.012	0.132 ± 0.011	0.121 ± 0.011	0.106 ± 0.010	0.104 ± 0.010

(*) The quoted errors are statistical only.

(**) The symbol $\overline{\Phi}_n$ represents the mean value of $\Phi_n(k,A_t)$ in the energy range 0.3 - 1.0 GeV.

Table 5 - Calculated (γ,n) Reaction Cross Sections (mb) (*).

k(GeV)	^{12}C	^{19}F	^{23}Na	^{55}Mn	^{103}Rh	^{197}Au	^{238}U
0.20	0.12 ± 0.03	0.15 ± 0.05	0.17 ± 0.06	0.29 ± 0.10	0.75 ± 0.26	2.08 ± 0.73	0.81 ± 0.47
0.25	0.43 ± 0.12	0.62 ± 0.19	0.73 ± 0.22	1.55 ± 0.46	1.33 ± 0.40	5.00 ± 1.50	6.13 ± 1.70
0.30	0.94 ± 0.25	1.34 ± 0.33	1.61 ± 0.40	3.46 ± 0.86	5.77 ± 1.44	10.09 ± 2.52	12.14 ± 3.00
0.32	1.04 ± 0.25	1.49 ± 0.37	1.79 ± 0.45	3.57 ± 0.94	6.34 ± 1.58	10.50 ± 2.62	12.15 ± 3.00
0.35	0.89 ± 0.25	1.32 ± 0.33	1.62 ± 0.40	3.61 ± 0.90	5.99 ± 1.49	10.51 ± 2.62	12.30 ± 3.00
0.40	0.62 ± 0.17	0.88 ± 0.21	1.06 ± 0.25	2.90 ± 0.70	4.25 ± 1.02	7.42 ± 1.78	9.09 ± 2.00
0.45	0.51 ± 0.17	0.76 ± 0.18	0.93 ± 0.22	2.05 ± 0.49	3.44 ± 0.83	6.82 ± 1.64	8.32 ± 2.10
0.50	0.39 ± 0.09	0.56 ± 0.12	0.60 ± 0.13	1.56 ± 0.34	2.67 ± 0.59	4.82 ± 1.06	5.75 ± 1.24
0.55	0.44 ± 0.13	0.67 ± 0.15	0.82 ± 0.18	1.82 ± 0.40	3.28 ± 0.72	5.84 ± 1.28	5.80 ± 1.20
0.60	0.47 ± 0.13	0.70 ± 0.15	0.86 ± 0.19	1.83 ± 0.40	3.33 ± 0.73	5.66 ± 1.25	6.26 ± 1.20
0.65	0.45 ± 0.13	0.70 ± 0.15	0.82 ± 0.18	1.69 ± 0.37	3.04 ± 0.67	5.08 ± 1.12	6.10 ± 1.20
0.70	0.51 ± 0.14	0.77 ± 0.19	0.92 ± 0.23	1.91 ± 0.48	3.43 ± 0.86	5.63 ± 1.40	6.57 ± 1.20
0.80	0.50 ± 0.14	0.78 ± 0.19	0.94 ± 0.23	1.91 ± 0.48	3.20 ± 0.80	5.42 ± 1.11	6.31 ± 1.20
1.00	0.39 ± 0.11	0.56 ± 0.17	0.69 ± 0.20	1.38 ± 0.41	2.44 ± 0.73	4.88 ± 1.46	4.32 ± 1.30
$\bar{\sigma}_{MC}$ (**)	0.54 ± 0.13	0.80 ± 0.16	0.96 ± 0.20	2.00 ± 0.43	3.57 ± 0.75	6.28 ± 1.20	6.94 ± 1.20

(*) The cross sections listed in this Table were calculated from Eq. 24. The quoted errors result from a combination of errors in the elementary cross sections and in the (γ,n) reaction probabilities (see Table 4).

(**) The symbol $\bar{\sigma}_{MC}$ represents the mean value of the cross sections in the energy range 0.3 - 1.0 GeV.

Table 6 - Comparison Between Experimental and Calculated Mean (γ,n) Reaction Cross Sections (mb) at Intermediate Energies.

Target Nucleus	Experimental Cross Section		Calculated Cross Sections			
	Ref.	$\bar{\sigma}_k$	$\bar{\sigma}_F$(Eq. 4)	$\bar{\sigma}_{MC}$(Table 5,Eq.24)	$\bar{\sigma}_{MC}$(Eq.25)	$\bar{\sigma}_c$(Eq.38)
^{12}C	12	0.85 ± 0.10				
	13	0.4 ± 0.1				
	15	1.18 ± 0.20	0.74 ± 0.09	0.54 ± 0.13	0.53	0.52
	21,27	0.6 ± 0.1				
	32	0.9 ± 0.1				
^{14}N	23	0.11 ± 0.05	0.85		0.61	0.59
^{16}O	23	0.6 ± 0.1	0.95		0.68	0.66
	29	1.27 ± 0.20				
^{19}F	23	0.42 ± 0.10				
	24	1.33 ± 0.20	1.11 ± 0.15	0.80 ± 0.16	0.79	0.77
	30	1.30 ± 0.10				
^{23}Na	30	1.60 ± 0.20	1.3 ± 0.2	0.96 ± 0.20	0.93	0.90
^{31}P	23	0.9 ± 0.1	1.70		1.21	1.17
	33	1.6 ± 0.1				
^{52}Cr	33	2.5 ± 0.5	2.69		1.88	1.83
^{55}Mn	17	7.7 ± 0.5				
	31	4.2 ± 0.6	2.8 ± 0.4	2.0 ± 0.4	1.98	1.91
	33	3.5 ± 0.5				
^{59}Co	18	3.3 ± 0.5	3.00		2.10	2.04
	33	3.0 ± 0.5				
^{75}As	22	8.7 ± 1.0	3.71		2.58	2.51
	33	4 ± 1				
^{103}Rh	19	13 ± 5	4.90 ± 0.75	3.57 ± 0.75	3.39	3.35
^{127}I	14	10 ± 6				
	20	4 ± 2	5.89		4.06	3.94
	33	5 ± 2				
^{197}Au	25	4 ± 2	9 ± 1	6.28 ± 1.20	5.92	5.74
	33	8 ± 3				
^{238}U	26	10 ± 5	10 ± 2	6.94 ± 1.20	6.97	6.76

FIGURE CAPTIONS

Fig. 1 - The experimental (γ,n) cross sections versus the mass number of the target nucleus, A_t. The straight line is a least squares fit of the experimental points. The shaded area represents two times the statistical error. The dashed line represents an extrapolation up to $A_t=1$. Experimental data are taken from: △ , Ref. [12]; ▲ , Ref. [13]; ▼ , Ref. [14]; □ , Refs. [15,19,24,26]; ▽ , Refs. [17,18,20-23,25,27]; ○ , Refs. [29,30,32]; ◇ , Ref. [31]; ● , Ref. [33].

Fig. 2 - Block diagram of the course of the Monte Carlo calculation of photonuclear cascades.

Fig. 3 - The (γ,n) probability, $\Phi_n(k,A_t)$, versus incident photon energy. The points represent the results of the present Monte Carlo calculation. For the sake of simplicity, only the (γ,n) probabilities for ^{12}C and ^{238}U are shown. The curves are eye fits through the calculated points.

Fig. 4 - Plot of the mean value of the (γ,n) probability, $\bar{\Phi}_n(k,A_t)$, in the energy range 0.3-1.0 GeV, versus the mass number of the target nucleus, A_t. The points have been calculated from the values listed in Table 4. The full line is a least squares fit of the calculated points. The dashed line represents an extrapolation up to $A_t=1$. The symbol ⧗ represents the ratio of the cross section of the $\gamma + p \rightarrow n + \pi^+$ reaction to the total inelastic cross section. The symbol ⧓ represents the ratio of the cross section of the $\gamma + n \rightarrow n + \pi^0$ reaction to the total ine

lastic cross section.

Fig. 5 - Trends of the (γ,n) reaction cross sections as a function of incident photon energy. The points are taken from Table 5 (for the sake of clearness only the cross sections of ^{238}U and ^{12}C are shown). The full lines are eye fits through the calculated points. For comparison, it is also shown the experimental trend for ^{12}C as reported by Andersson et al. [27] (dashed line).

Fig. 6 - A_t-dependence of the (γ,n) mean cross section, $\bar{\sigma}_{MC}$. The points are the calculated cross sections listed in Table 5. The straight line marked $A_t^{0.86}$ is a least squares fit of the calculated points. For the sake of comparison, the trends are also reported for a surface production model ($A_t^{2/3}$) and a volume production model (A_t^1).

Fig. 7 - The energy-dependence of the (γ,n) reaction probability, $\eta(k)$. (For details see text). The points are calculated values of η/k. The straight line was obtained by least squares fit. The error bars are statistical uncertainties.

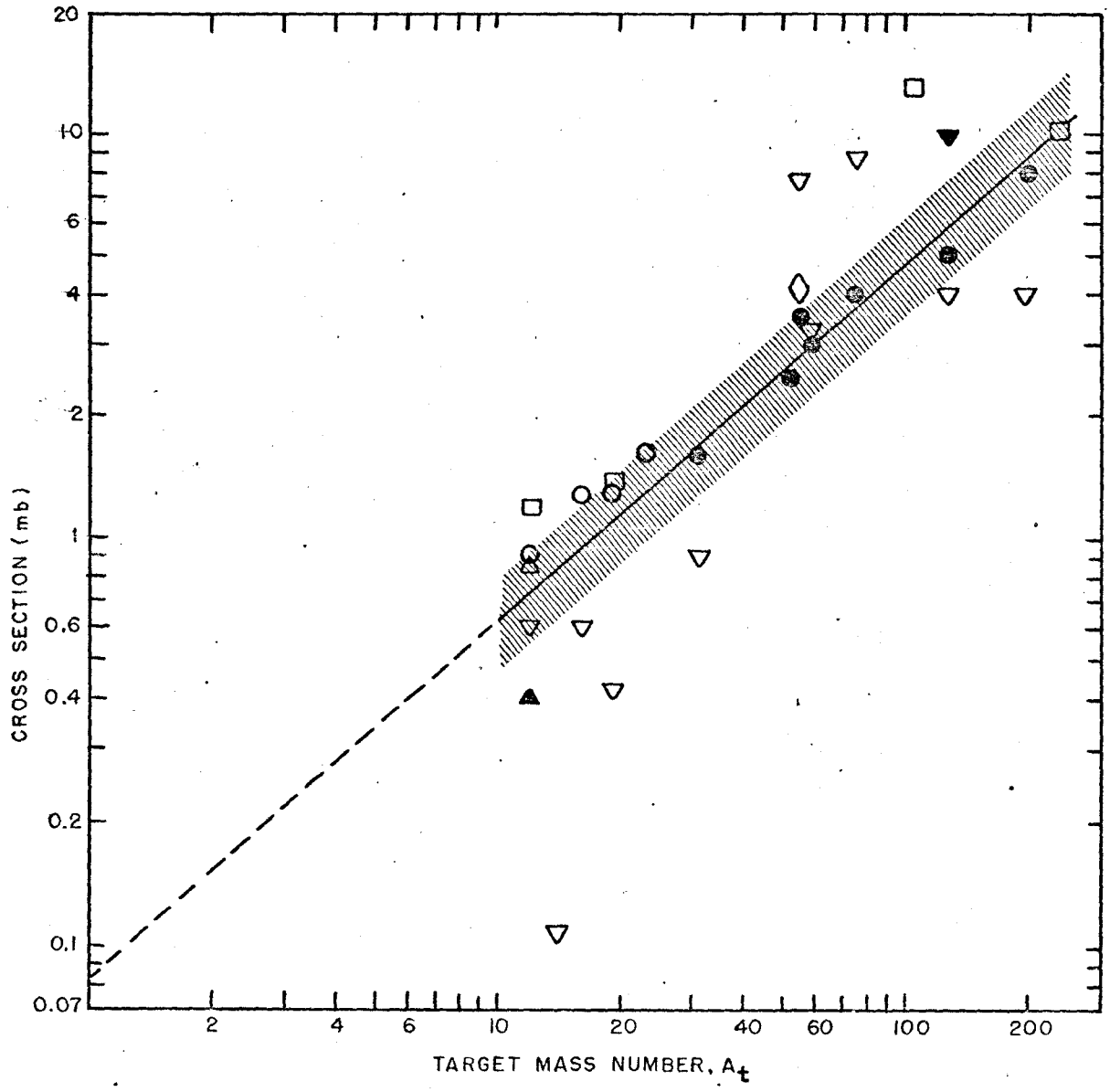
20
10
6
4
2
1
0.6
0.4
0.2
0.1
0.07
CROSS SECTION (mb)
2
4
6
10
20
40
60
100
200
TARGET MASS NUMBER, A_t

Figure 1

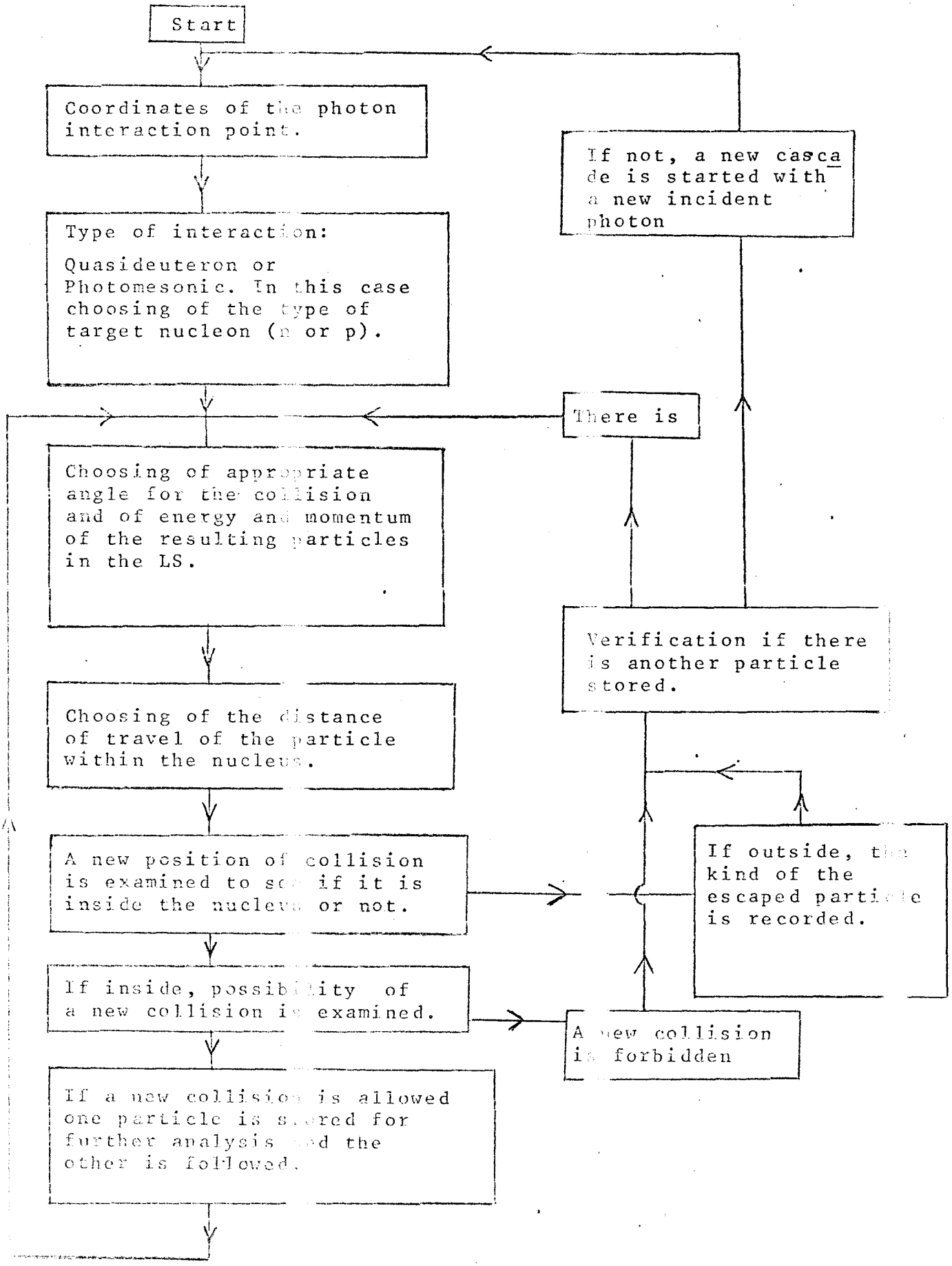
Start
Coordinates of the photon interaction point.
Type of interaction:
Quasideuteron or Photomesonic. In this case choosing of the type of target nucleon (n or p).
Choosing of appropriate angle for the collision and of energy and momentum of the resulting particles in the LS.
Choosing of the distance of travel of the particle within the nucleus.
A new position of collision is examined to see if it is inside the nucleus or not.
If inside, possibility of a new collision is examined.
If a new collision is allowed one particle is stored for further analysis and the other is followed.
A new collision is forbidden
If outside, the kind of the escaped particle is recorded.
Verification if there is another particle stored.
There is
If not, a new cascade is started with a new incident photon

Figure 2

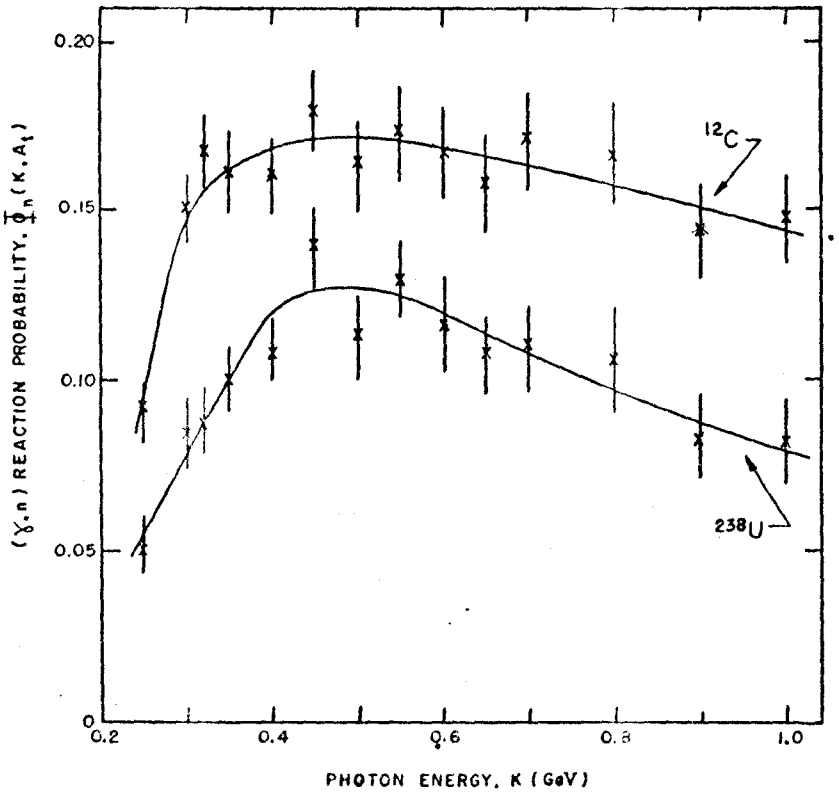

Figure 3

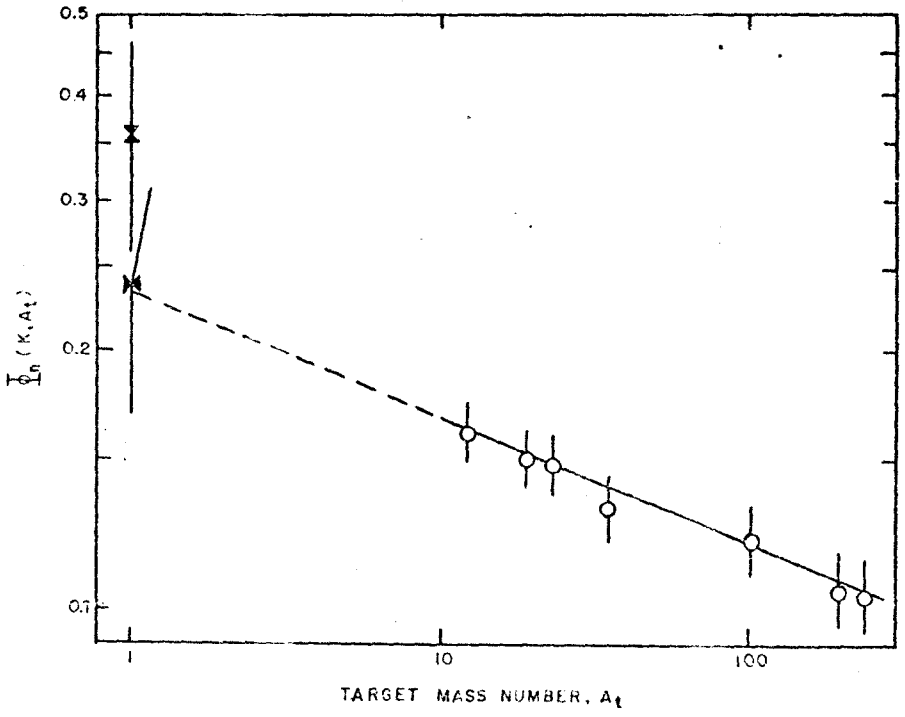

Figure 4

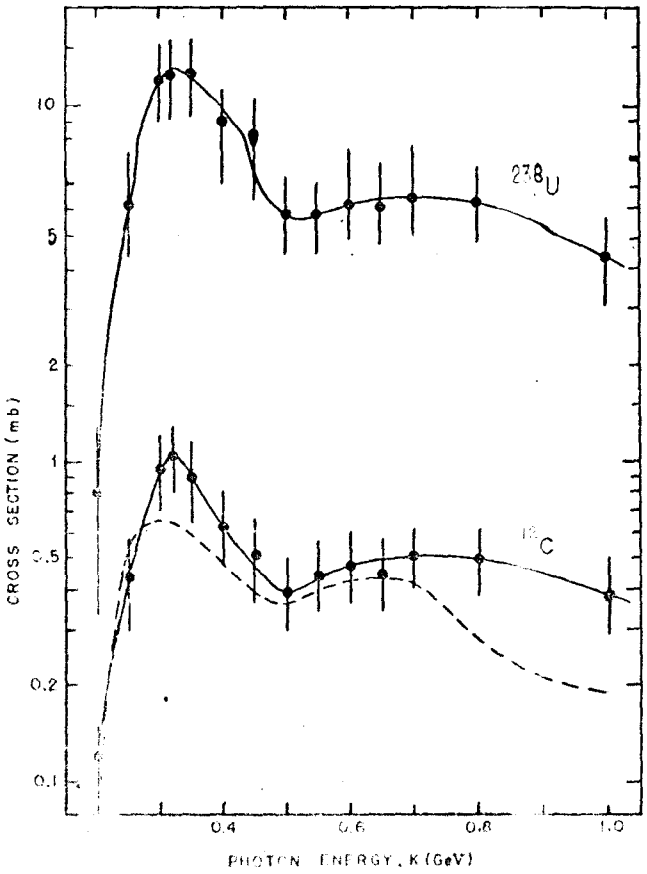

Figure 5

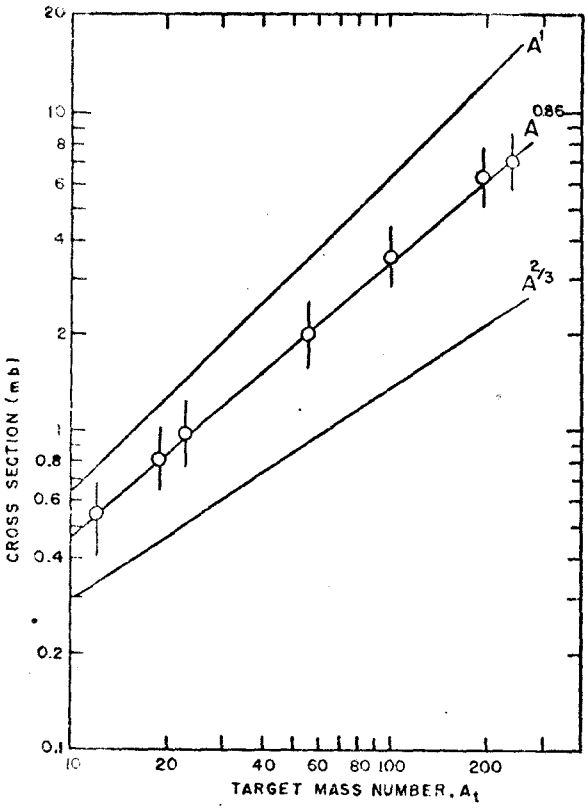

Figure 6

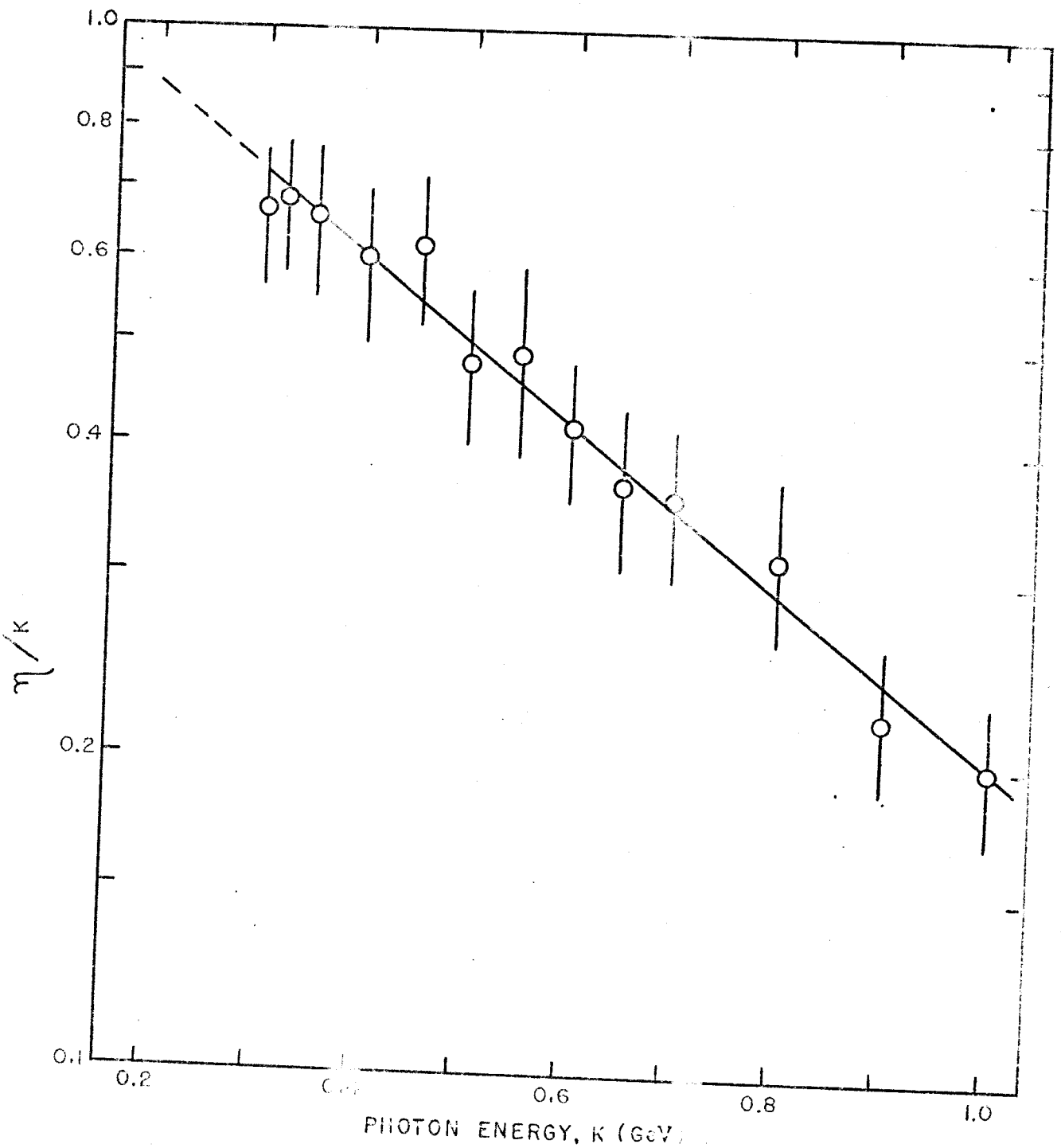

Figure 7